INTERNATIONAL JOURNAL OF CURRENT RESEARCH IN CHEMISTRY AND PHARMACEUTICAL SCIENCES
(p-ISSN: 2348-5213: e-ISSN: 2348-5221)
www.ijcrcps.com
Coden:IJCROO(USA–American Chemical Society)

Research Article

SOI: http://s-o-i.org/1.15/ijcrcps-2015-2-11-10

PROTIC IONIC LIQUID ASSISTED SYNTHESIS AND CHARACTERIZATION STUDIES OF CHALCOGEN AND CHALCOGENIDE NANOPARTICLES

DR.L. MEGALA[1*] AND K. KAMALAKANNAN[1]

[1*]Department of Chemistry, A.D.M. College for women (Autonomous), Nagapattinam,Tamilnadu, India -611 001.
[1]Department of Chemistry, A.D.M. College for women (Autonomous), Nagapattinam,Tamilnadu, India -611 001.
*Corresponding Author: lmadmc2016@gmail.com

Abstract

Recently, nanoparticle synthesis employing ILs emerges as a new attention in the field of green chemistry especially, ILs with imidazolium cation. ILs with the general characteristics of low interfacial tension permits in adapting to the surrounding reaction media and their relative solubility can be tuned by varying their anionic and cationic components**.** Green synthesis of selenium(chalcogen) nanoparticles (SeNPs) attained using simple wet chemical method involved in the reactions of six types of protic ionic liquids with imidazolium cations and sodium hydrogen selenide (NaHSe) in the presence of poly ethylene glycol-600(PEG-600) as an additional stabilizer. The acquired SeNPs were characterized using UV, IR, XRD, TGA, DTA SEM with EDAX and TEM analysis. Using the synthesized SeNPs, two chalcogenides such as ZnSe and CdSe semiconductor nanoparticles were prepared and characterized using XRD, SEM with EDAX and TEM analysis.

Keywords: nanoparticle, SeNPs, UV, IR, XRD, TGA, DTA SEM with EDAX and TEM analysis.

1. INTRODUCTION

The synthesis and stabilization of metal nanoparticles (M-NPs) from metals, metal salts, metal complexes and metal carbonyls in ionic liquids (ILs) is reviewed. . ILs can be divided into two broad categories: protic ILs (PILs) and aprotic ILs (APILs). PILs are produced through proton transfer from a Bronsted acid to a Bronsted base. Historically, the first PIL, EOAN was reported in 1888 by Gabriel [1]. There are a large number of reports on the properties of APILs and their applications in different fields [2-8]; however, there are few reviews on PILs [9]. In comparison with APILs, PILs often have higher conductivity and fluidity as well as lower melting points [10]. They are also cheaper and more convenient to prepare as their synthesis does not involve the formation of byproducts [9]. Normally, PILs are prepared through the neutralization of a base by an acid [11, 12] or the mixture of equimolar amounts of acid and base [10,13]. Ideally, the proton transfer is completed from Bronsted acid to Bronsted base, but, in most cases, a neutral species is formed owing to incomplete proton transfer. Aggregation or the formation of ion complexes also can happen to prevent complete proton transfer, which limits the ionicity of the PILs . Normally, proton transfer improves by using stronger acids and bases. PILs have wide applications in biological systems and chromatography [14]. In addition, they have been applied as proton-conducting electrolytes for polymer membrane fuel cells [15-19], because of the advantage of having a defined proton activity as well as high proton conductivity, allowing the fuel cell to operate under non humidified and high-temperature conditions. The precursor haloalkanes must be initially washed with portions of concentrated sulphuric acid then neutralized with a sodium bicarbonate ($NaHCO_3$) solution and deionized water, and finally distilled before use. Sublimation of aluminium chloride ($AlCl_3$) prior to use will facilitate to obtain colorless ILs based on $AlCl_3$. Conventional molten salts

such as sodium chloride, lithium chloride exhibit a high melting point [801^{0}C and 614^{0}C respectively] which limits their use as solvents in most applications. ILs can beused as green solvents and stabilizers for nanoparticles (NPs) due to their general ease of synthesis, stability (nonflammable, thermally stable), and low vapor pressure. Many nanostructured materials are synthesized using ILs as precursors. ILs with imidazolium cation comprises pre-organized structures via hydrogen bonds that bring structural directionality. Pure selenium along with selenium containing nanomaterials possesses admirable photoelectrical characteristics, semiconductor properties and high biological activity [20]. Nano-selenium possess large piezoelectric, high photoconductivity, thermoelectric and non-linear responses and used in photocells, photographic exposure meters, xerography.electrical rectifiers etc., [21]. The amorphous selenium nanoparticles contain unique photoelectric, semiconducting and x-ray-sensing properties [22]. It possess high reactivity and leads to a variety of functional materials like Ag_2Se [23], CdSe [23], ZnSe [24] and PbSe [24]. Hence the selenium nanoparticle has a scope of research. This paper imparts a new path for the synthesis of SeNPs by the reaction of sodium hydrogen selenide with each of six PILs 2-methylimidazolium lactate ([Hmim]$CH_3CH(OH)COO^-$), 1-ethylimidazolium lactate ([Heim]$CH_3CH(OH)COO^-$), 1-butylimidazolium lactate([Hbim] $CH_3CH(OH)COO^-$), 2-methylimidazolium glycolate([Hmim]$CH_2(OH)COO^-$),1-ethylimidazolium glycolate([Heim] $CH_2(OH)COO^-$),1-butylimidazolium glycolate([Hbim] $CH_2(OH)COO^-$) individually in the presence of PEG-600 as additional stabilizer. By the reaction of selenium with $NaBH_4$, NaHSe was obtained. By making use of one of the synthesized SeNPs as precursor ZnSe and CdSe nanoparticles were synthesized. The ZnSe and CdSe were the useful semiconductors containing a wide optical band gap.

2. Experimental

2.1. Materials

2-methylimidazole,1-ethylimidazole,1-butylimidazole,lactic acid ,glycolic acid ,selenium powder,sodium borohydride,polyethylene glycol -600 (PEG-600)were purchased from Sigma–Aldrich and utilized exclusive of further purification.Cadmium sulphate and Zinc acetate with AR quality were also purchased.

2.2. Synthesis of imidazoliumprotic ionic liquids

The protic ionic liquids were synthesized by mixing the equimolar ratio of the precursor bronsted acids (hydroxy carboxylic acids) and bronsted bases (substituted imidazoles) taken in a reaction vessel using a magnetic stirrer for an hour and subjected to microwave irradiation in a determined period of time and power level [25].(scheme1).

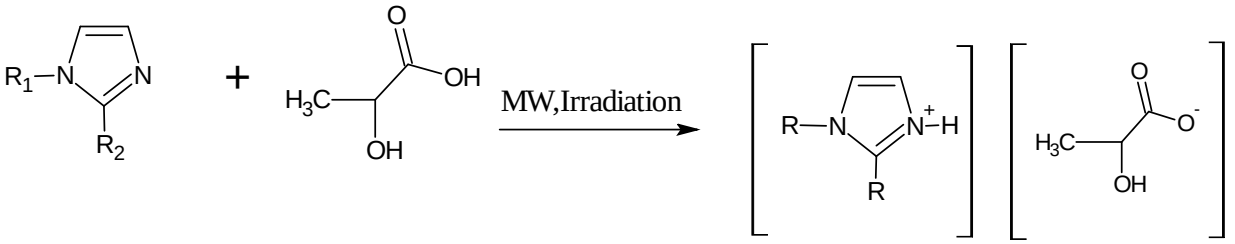

Lactic acidProtic ionic liquids

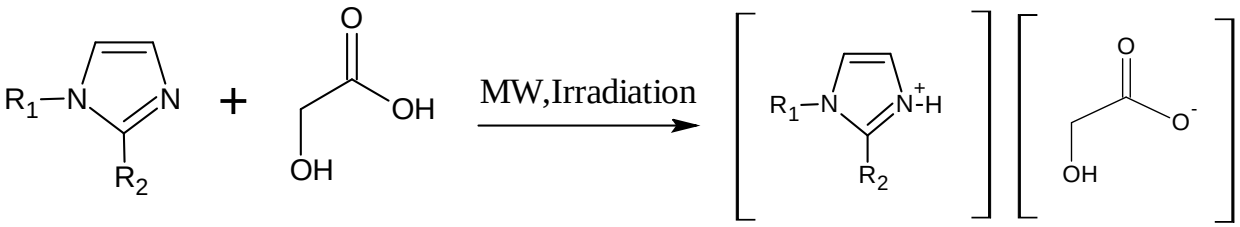

Glycolic acidProtic ionic liquids

where **R_1**-H,C_2H_5- or C_4H_9-.
R_2-H,CH_3

Scheme–1. The protic ionic liquids were synthesized by mixing the equimolar ratio of the precursor bronsted acids (hydroxy carboxylic acids) and bronsted bases (substituted imidazoles)

2.3. Preparation of Sodium hydrogen Selenide

A mixture of 1gm of selenium powder, 3gm of $NaBH_4$ and 15ml of deionized water in a reaction vessel was stirred well and heated to 40^0C for an hour. The resulting homogeneous solution of sodium hydrogen selenide was washed with excessive water.

.

$$4\ NaBH_4 + 2Se + 7\ H_2O \rightarrow 2NaHSe + Na_2B_4O_7 + 14\ H_2 \quad \text{----------}>1$$

2.4. Synthesis of SeNPs

The aqueous solution of sodium hydrogen selenide and 1 ml of PEG-600 was added with 5ml of [2mim] $CH_3CH(OH)COO^-$. For nearly 6 hours the reaction mixture was stirred at 80^0C using a magnetic stirrer later cooled down and kept at room temperature (27^0C) for 24hrs. Using centrifugation the SeNPs deposited in the bottom of the reaction vessel were recovered.

The above said process is performed for the left over PILs like [Heim]$CH_3CH(OH)COO^-$,[Hbim] $CH_3CH(OH)COO^-$,[Hmim]$CH_2(OH)COO^-$,[Heim] $CH_2(OH)COO^-$,[Hbim] $CH_2(OH)COO^-$ separately in a different reaction vessels.

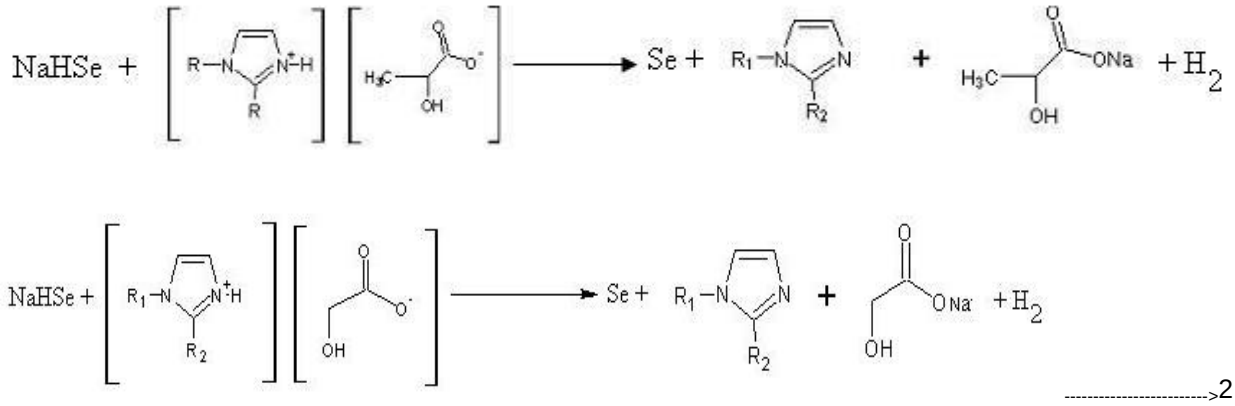

----------->2

Scheme - 2

2.5. Preparation of CdSe Nanoparticles

0.2 g of $CdSO_4$ in 10 ml of deionised water was added with the solution of 0.2g of SeNPs (synthesized using [Hbim] $CH_2(OH)COO^-$ which stabilizes the SeNPs to a larger extend than rest of the PILs) in 2ml [Hbim] $CH_2(OH)COO^-$ and 1ml of PEG-600.The obtained mixture was stirred for 6 hours using a magnetic stirrer at 60^oC . The black precipitate of CdSe was extracted and washed with ethanol and hot distilled water several times.

2.6. Preparation of ZnSe Nanoparticles

The mixture of zinc acetate (0.2g), 10ml of deionized water and 0.2g of SeNPs (synthesized using [Hbim] $CH_2(OH)COO^-$) was stirred well for 3hrs and later heated to 120^oC for a period of 2hrs. The black precipitate of ZnSewas extracted and washed several times with acetone and hot distilled water.

2.7. Characterization

The absorption spectrum were recorded by Perkin Elmer Lambda35 Spectrometer and the energy band gap was calculated using the direct formula E_g^0 (eV) = 12397.8 /λ_{max}(Å) where E_g^0 is the energy band gap and λ_{max} is the wavelength at which maximum absorption was shown. The FT-IR spectra were recorded using the Jasco (FT-IR 460) spectrometer. XRD was carried out by XPERT – PRO diffractometer which utilizes Cu–Kα (1.5406 Å).SEM and TEM images were obtained using VEGA3-TESCAN Jeol/JEM 2100instrument. The TGA and DTA measurements were performed using PerkinElemer/TGA4000 analyzer.

3. RESULTS AND DISCUSSION

3.1. Selenium nanoparticles (SeNPs)and CdSe,ZnSe nanoparticles

All the synthesized protic ionic liquids were noted acidic in nature [25].Sodium hydrogen selenide was decomposed in the ionic liquids (acidic medium) in the presence of PEG-600 to yield SeNPs as shown in equation-2. The course of reaction involved in the transfer of proton from PILs and reacted with NaHSe to produce elemental SeNPs as shown in scheme-2. Subsequently these nanoparticles were coated by the [Hbim] $CH_2(OH)COO^-$ ionic liquid and this coating impedes further growth of the particles. Furthermore the low interfacial tension of ionic liquids led to high nucleation rates and enabled the generation of small nanoparticles[26]. Additionally the high viscosity of surrounding medium (ionic liquids with η=1216cP) minimizing the probability of close contacts of nanoparticles thereby inhibiting the growth of particles and resulting the selenium nanoparticles with smaller in size.

The PIL([Hbim] $CH_2(OH)COO^-$) that acted not only as a reducing agent but also as a stabilizer in the formation of CdSe and ZnSe nanoparticles. The first step of both the cases involved the reduction of elemental SeNPs to Se^{2-} ions by [Hbim] $CH_2(OH)COO^-$. The so formed selenide ions react with Cd^{2+} (from Cadmium sulphate) and Zn^{2+} (from Zinc acetate) resulting CdSe and ZnSe respectively with a higher yield(**Scheme -3and Scheme - 4).**

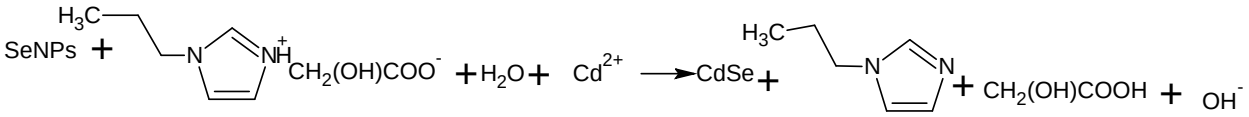

Scheme - 3

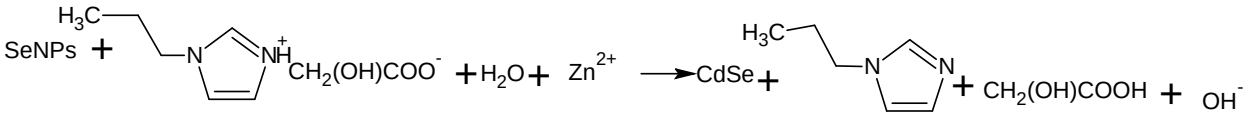

Scheme - 4

Later the resulting CdSe and ZnSe nanoparticles were electrostatically stabilized using [Hbim] $CH_2(OH)COO^-$. The $[Hbim]^+$ cations of [Hbim] $CH_2(OH)COO^-$were combined with selenide moieties of CdSe and ZnSe through electrostatic attraction and forms a layer around nanoparticles. As a result, the surrounding layer formed by $[Hbim]^+$ hindered the agglomeration of the obtained CdSe and ZnSe nanoparticles in the solution resulting in smaller size particles. In the absence of PIL, small sized CdSe and ZnSe nanoparticles grow and form CdSe and ZnSe aggregates respectively with a larger size .Hence the rate for nucleation of nanoparticles prepared in presence of the PIL is higher than the prepared sample in other aqueous solutions.

3.2. UV-Spectral Studies

The strong absorption bands possessing absorption maximum 262.9, 223.9, 217.9, 259.47, 221.8,213.69nm with transmittance ranging from0.2740 - 0.5269 were observed for SeNPs obtained from [Hmim]$CH_3CH(OH)COO^-$,[Heim]$CH_3CH(OH)COO^-$, [Hbim] $CH_3CH(OH)COO^-$, [Hmim]$CH_2(OH)COO^-$, [Heim] $CH_2(OH)COO^-$, [Hbim] $CH_2(OH)COO^-$ respectively. But the precursor selenium powder posses the absorption maximum of 431.96nm with the transmittance 0.1364 as shown in figure- 1.

Byidentifying the band gap energy of SeNPs the optical properties of SeNPs were determined. From the absorption peaks, the optical energy band gap was calculated using the formula E_g^0 (eV) = 12397.8 /λ_{max}(Å) [27] and compiled in table-1.It is obvious that the calculated band gap values of the SeNPs were blue shifted from the precursor selenium. Increasing the band gap energies of SeNPs procures an indication of the quantum confinement effect due to the decreasing size of particles. Owing to the size effect, the wide increase in band gap of about 2.8196eVwasattained when compared with precursor selenium (2.8701 eV)[28]

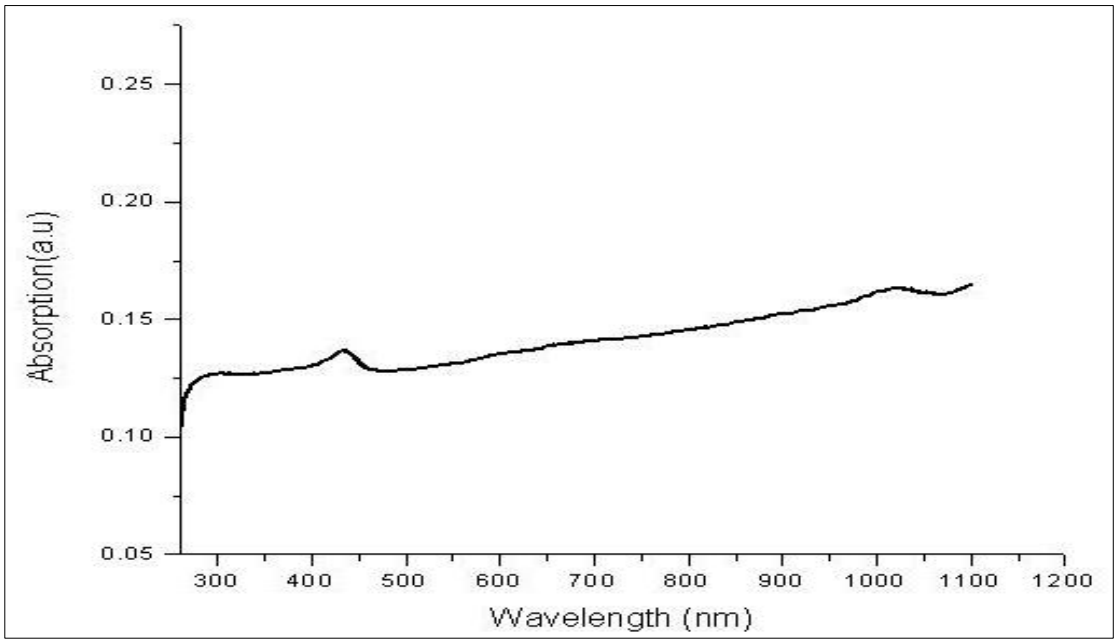

Figure 1- UV-absorption spectrum of precursor Se (i) and

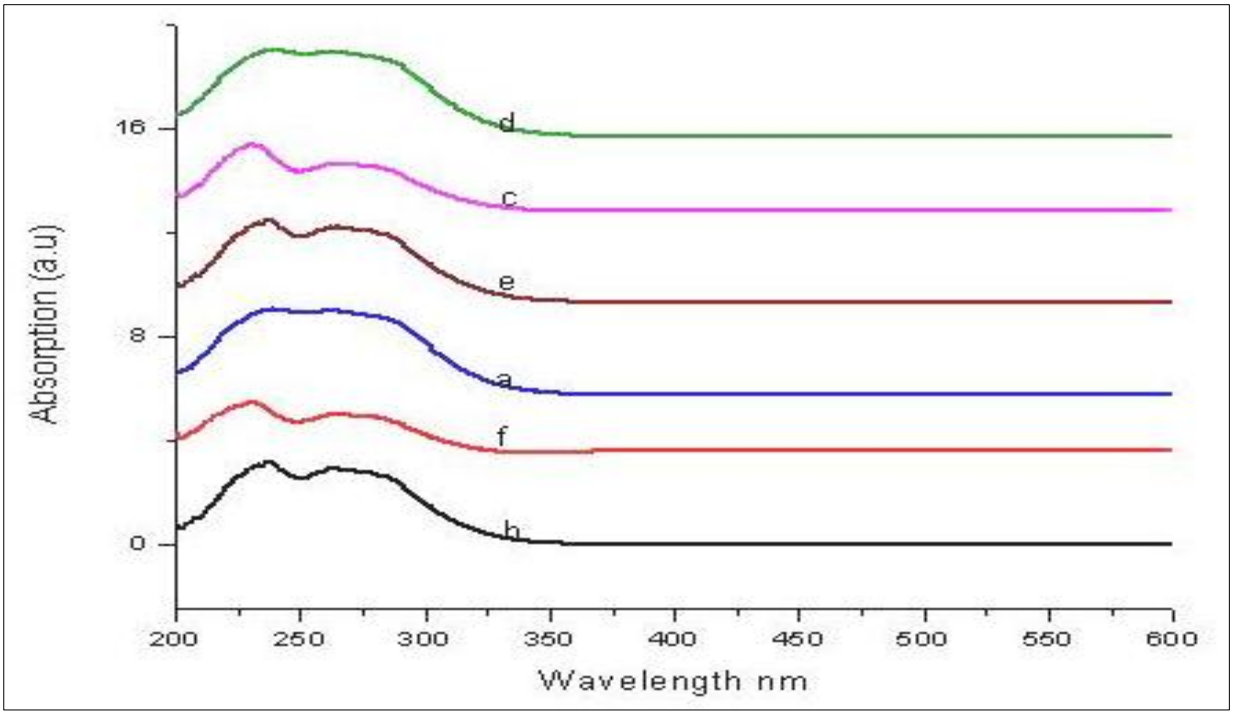

SeNPs (ii)

Where a,b,c,d,e,f are the SeNPS synthesized from [Hmim]$CH_3CH(OH)COO^-$) [Heim]$CH_3CH(OH)COO^-$,[Hbim]$CH_3CH(OH)COO^-$,[Hmim]$CH_2(OH)COO^-$,[Heim] $CH_2(OH)COO^-$, [Hbim] $CH_2(OH)COO^-$ respectively.

Table .1-Band gap energies of SeNPs

S.No	Content	Λmax(Å)	Band gap(eV)
1	Precursor se	4319.6	2.8701
2	A	2629.0	4.7158
3	B	2239.0	5.5372
4	C	2179.0	5.6897
5	D	2594.7	4.7781
6	E	2218.0	5.5896
7	F	2136.9	5.8018

Where a,b,c,d,e,f are the SeNPs synthesized from [Hmim]$CH_3CH(OH)COO^-$) [Heim]$CH_3CH(OH)COO^-$),[Hbim]$CH_3CH(OH)COO^-$),[Hmim]$CH_2(OH)COO^-$),[Heim] $CH_2(OH)COO^-$), [Hbim] $CH_2(OH)COO^-$) respectively.

3.3.FT –IR spectral Studies

The FT-IR spectrum of precursor selenium and SeNPs shown in figure-2.The FT-IR spectroscopy is effectively used to measure the particle formation [29].In the case of precursor selenium the prominent absorption peaks were obtained at3434cm^{-1},1594 cm^{-1},1384 cm^{-1},1352 cm^{-1},765 cm^{-1} whereas for SeNPs absorption peaks were at3401cm^{-1},1584 cm^{-1}, 1341 cm^{-1},761 cm^{-1}.Hence theFT-IR spectrum of SeNPs differs considerably from the precursor selenium in a bulk form. This distinguished feature exhibited by SeNPs is termed to the fact that, in the case of SeNPs the surface to volume ratio noted very high when compared to precursor selenium ina bulk form.

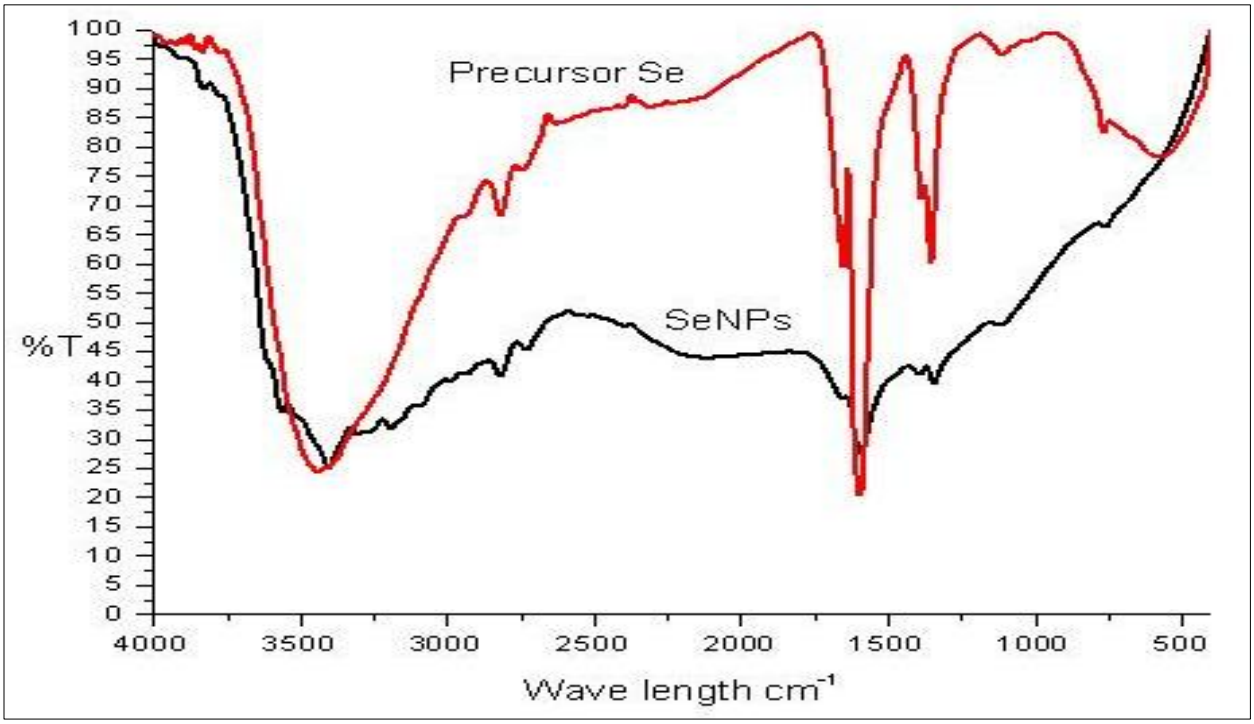

Figure 2- FT-IR Spectrum of precursor Se and SeNPs

Moreover figure-2 makes evident that the width and intensity of peaks in FT-IR spectrum were influenced more due to the particle size. The peaks of SeNPs had smaller intensity (smaller the percent transmittance) and narrow width

whereas the peaks of precursor selenium possess higher intensity (higher the percent transmittance) and broader width. Thus, as size of the particle decreases with an increase in the width of the peaks and decrease in the intensity. Thereby the formation of SeNPs was confirmed by FT-IR analysis.

3.4.X-ray diffraction analysis

The XRD pattern of the synthesized SeNPs shown in figure-3 matches well with the standard Se powder JCPDS CAS No.86-2246(figure-3)confirming the formation of SeNPs. The SeNPs containing hexagonal structure with lattice constants(a=4.4245 Å, c=5.0520 Å)were well in agreement with the literature values (a=4.368Å,c=4.958 Å).The average sizes of SeNPs using different PILs were calculated using Debye-Scherer equation and compiled in table-2. The SeNPs synthesized from [H1bim] $CH_3CH(OH)COO^-$),[Hbim] $CH_2(OH)COO^-$) possess a size of 20.4583 nm and 19.4439 nm(Table-2) respectively and smaller in size when compared to other SeNPs obtained from the rest of the PILs. Evident to the fact that the increased alkyl chain in imidazolium cation stabilized the SeNPs strongly resulting in smaller sized particles. Thus PILs acts also as a stabilizer, which predominantly resulting the nanoparticles with smaller in size. The smaller size nanoparticles were acquiredin more pre-organized ionic liquid structure.

The XRD pattern of the synthesized CdSe shown in figure-4.The XRD measurement of CdSe revealed that the position of the diffracted peak matches well with the standard powder diffraction data (a=4.299 Å, c=7.010 Å). Various peaks of CdSe 23.80,25.21,27.81,44.91,62.6 were obtained due to diffraction from (100),(002),(001),(103),(203) planes of hexagonal CdSe which were in a better agreement with hexagonal structure JCPDS CAS No.77-2307 (figure-5).From the different θ values, the calculated average particle size was noted about 29.97 nm.

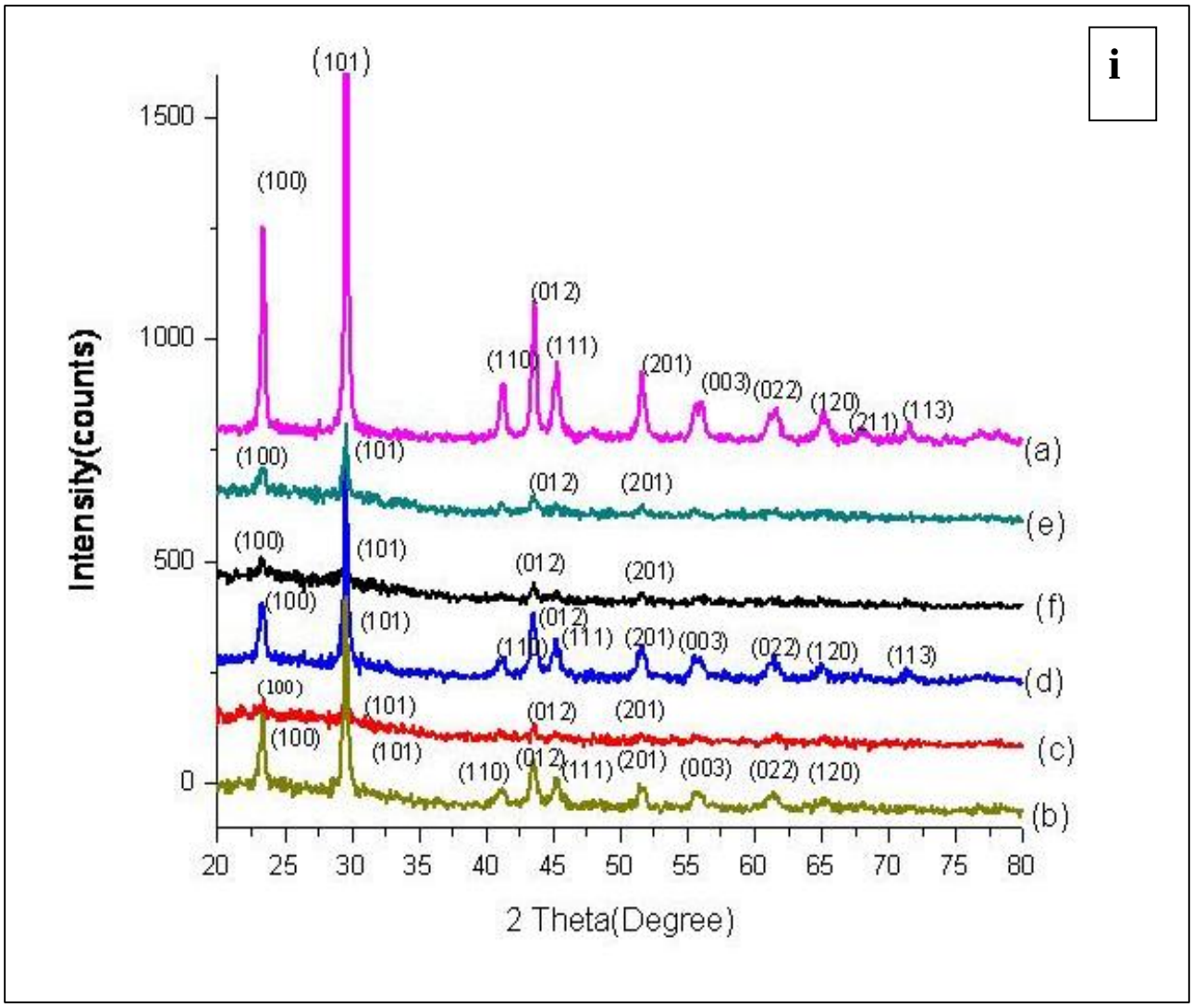

Figure 3.- XRD of Synthesised SeNPs(i) and Precursor selenium

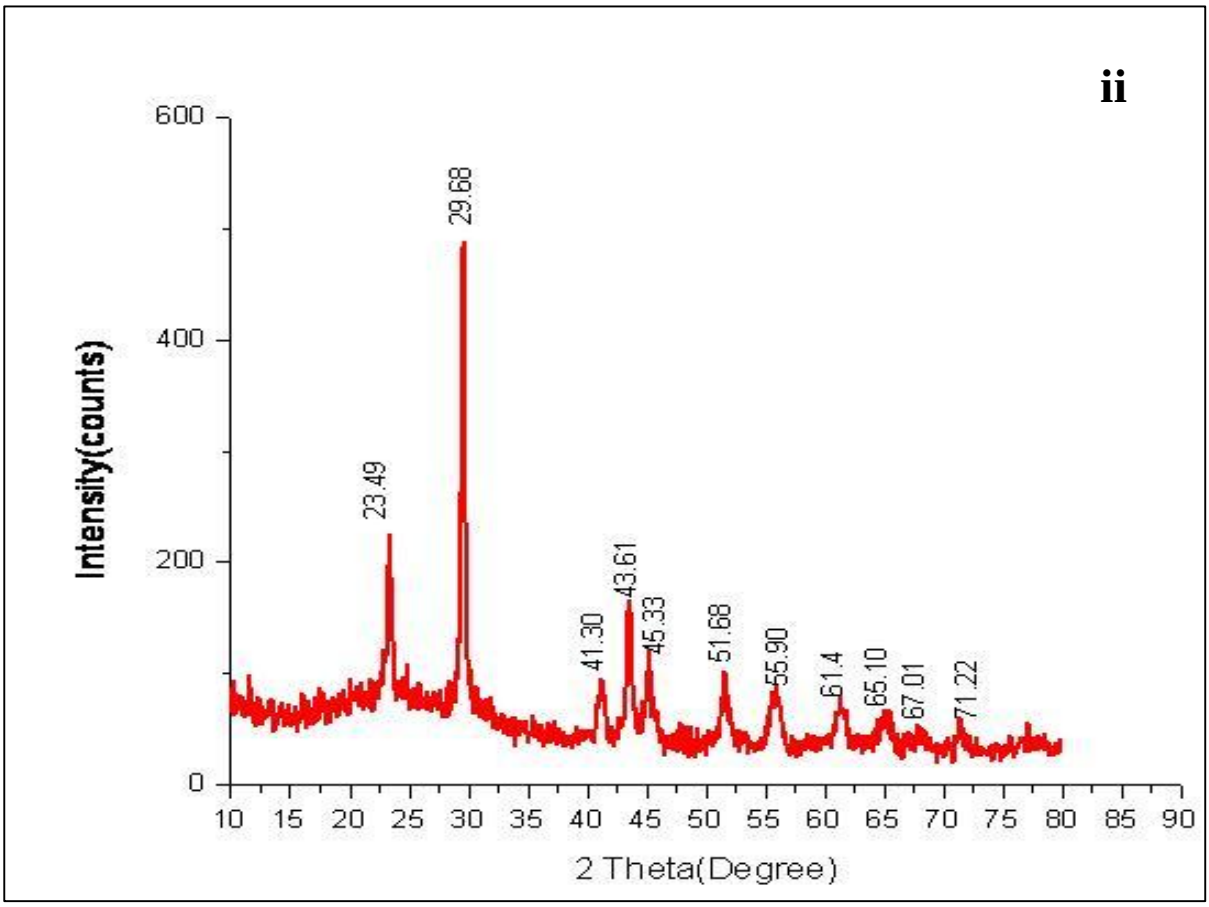

(ii), Where a,b,c,d,e,f are the SeNPs synthesized from [Hmim]$CH_3CH(OH)COO^-$, [Heim]$CH_3CH(OH)COO^-$, [Hbim]$CH_3CH(OH)COO^-$, [Hmim]$CH_2(OH)COO^-$, [Heim] $CH_2(OH)COO^-$, [Hbim] $CH_2(OH)COO^-$ respectively.

Table.2-XRD pattern for SeNPs

S.No	Content	2θ	hkl	Average Size (nm)
1	a	23.39, 29.59, 41.22, 43.56, 45.25, 51.59,55.55 ,61.4,65.08,67.9,71.2	(100), (101), (110), (012), (111), (201), (0 03), (022),(120),(211), (113)	24.2050
2	b	23.36,29.55,41.2,43.52,45.24,51. 6,55.7,61.3,65.1	(100), (101), (110), (012), (111), (201), (003), (022),(120)	23.9569
3	c	23.36,29.55,43.55,51.59	(100), (101), (012), (201)	20.4583
4	d	23.33,29.56,41.14,43.51,45.17,51 .55,55.77,61.32,65.11,71.19	(100), (101), (110), (012), (111), (201) (003), (022), (120),(113)	23.6071
5	e	23.2,29.57,43.55,52.2	(100), (101), (012), (201)	22.4732
6	f	23.31,29.53,43.51,51.58	(100), (101), (012), (201)	19.4439

Where a,b,c,d,e,f are the SeNPs synthesized from [Hmim]$CH_3CH(OH)COO^-$,[Heim]$CH_3CH(OH)COO^-$,[Hbim]$CH_3CH(OH)COO^-$,[Hmim]$CH_2(OH)COO^-$,[Heim] $CH_2(OH)COO^-$, [Hbim] $CH_2(OH)COO^-$ respectively.

From the XRD measurements of ZnSe (figure-6) it made clear that the position of the diffracted peak matches well with the standard powder diffraction data (a= 3.996 Å, c=6.626 Å). The several peaks of ZnSe 25.69,26.17,30.12,36.9,45.21 were acquired due to diffraction from(100),(002),(101),(102),(110) planes of hexagonal ZnSe which agree well with hexagonal structure JCPDS CAS No.89-2940(figure-7). From the different θ values, the calculated average particle size was noted about 22.73 nm.

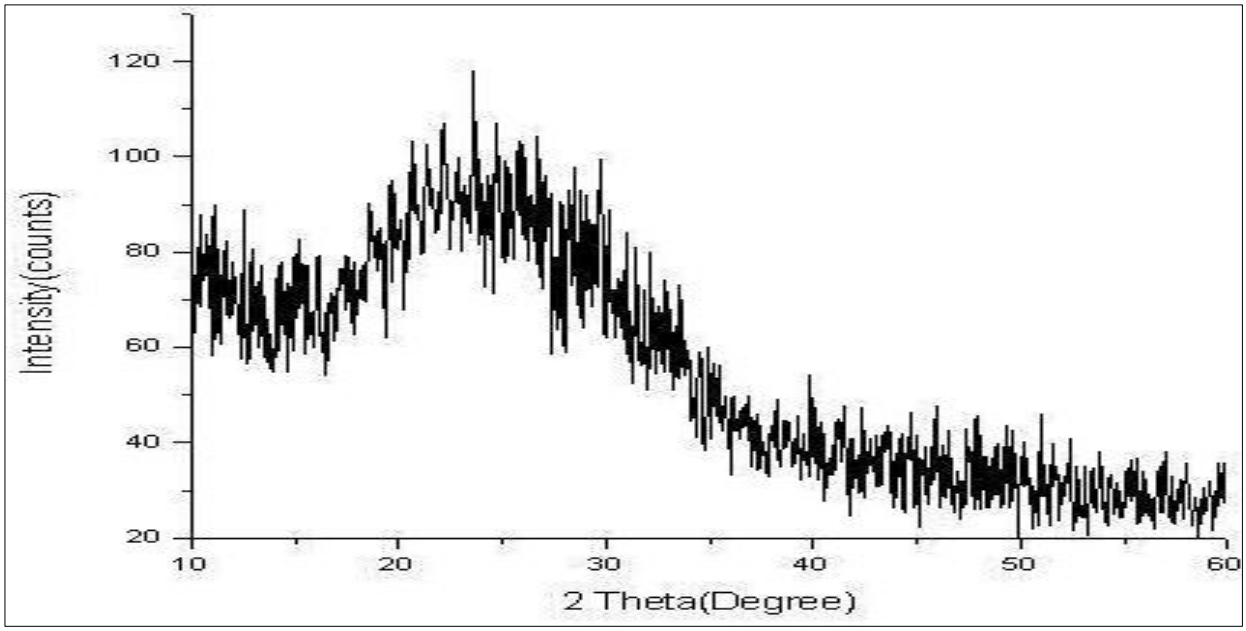

Figure.4- XRD pattern of synthesized CdSe

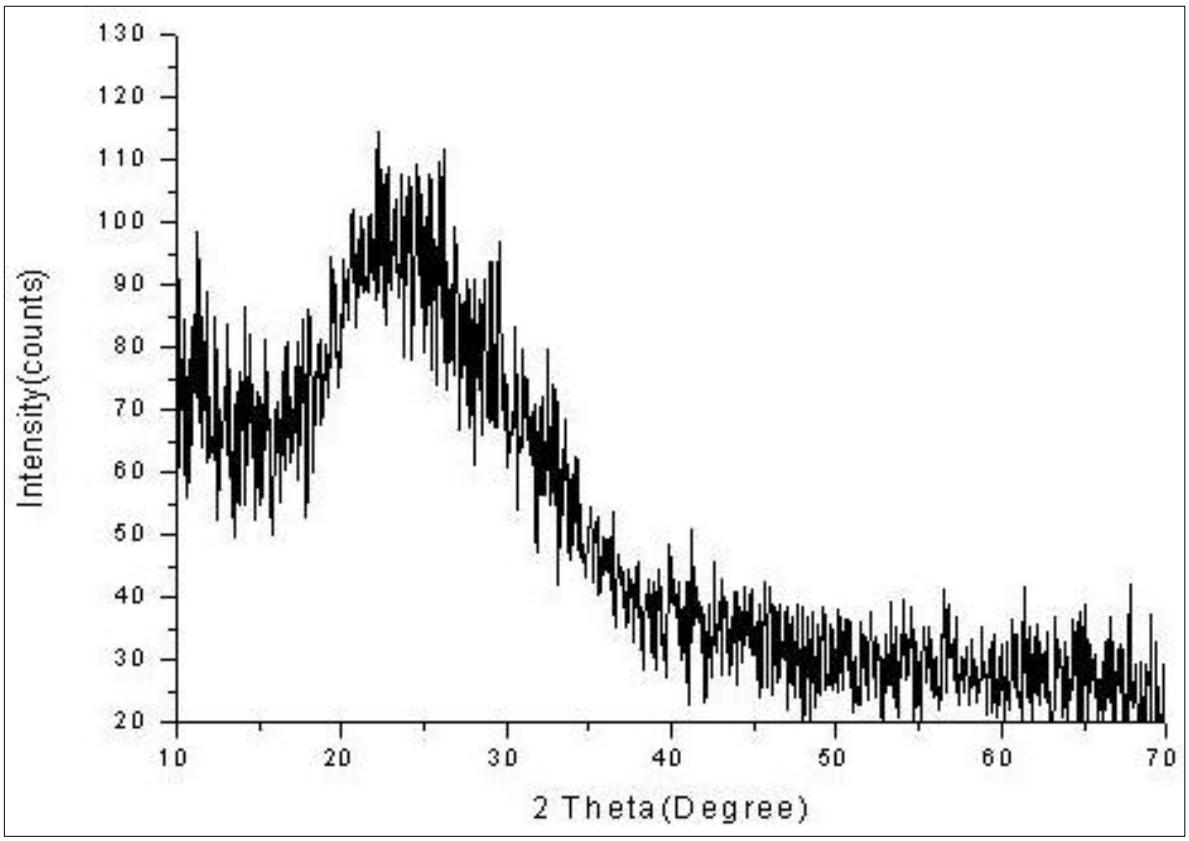

Figure.5- XRD pattern of synthesized ZnSe

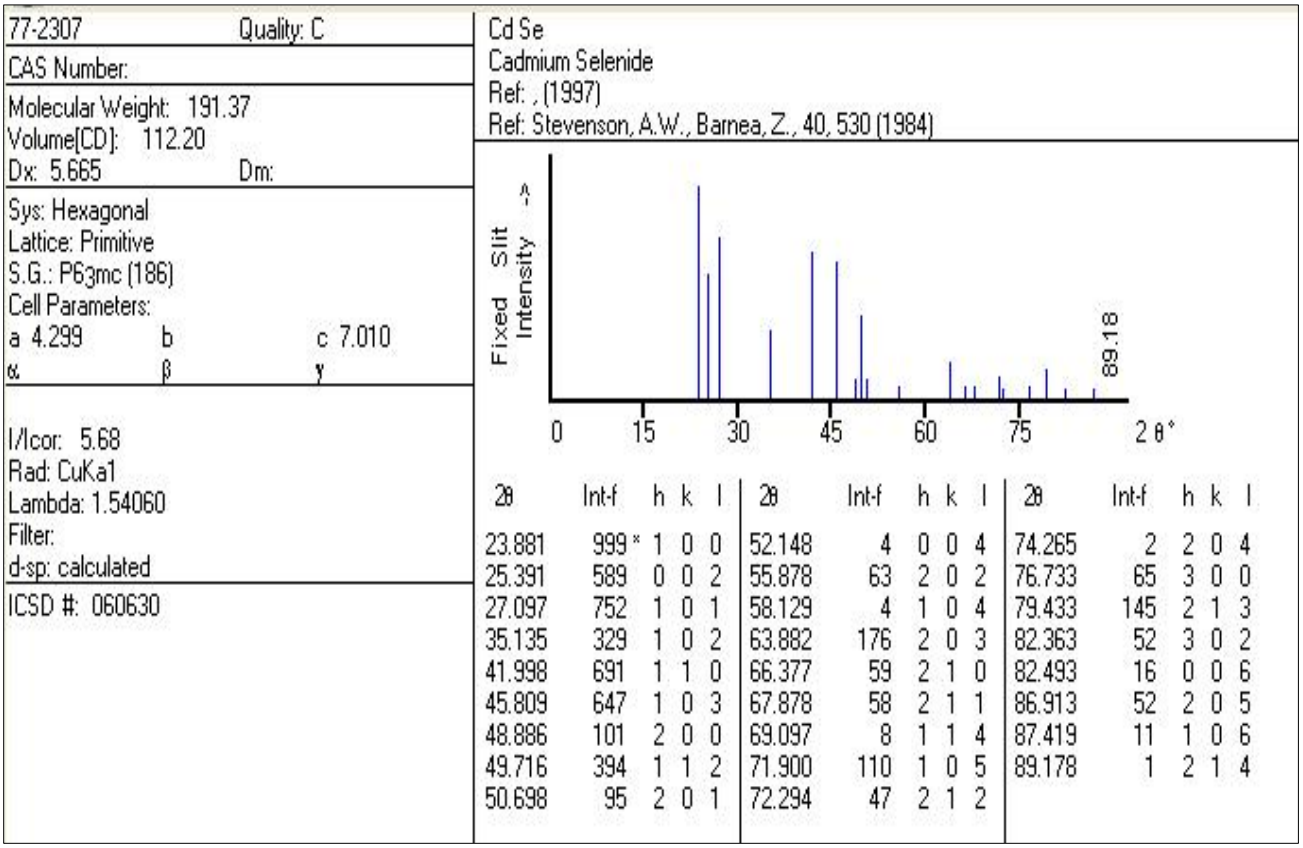

77-2307 Quality: C

CAS Number:

Molecular Weight: 191.37
Volume[CD]: 112.20
Dx: 5.665 Dm:

Sys: Hexagonal
Lattice: Primitive
S.G.: P63mc (186)
Cell Parameters:
a 4.299 b c 7.010
α β γ

I/Icor: 5.68
Rad: CuKa1
Lambda: 1.54060
Filter:
d-sp: calculated

ICSD #: 060630

Cd Se
Cadmium Selenide
Ref: , (1997)
Ref: Stevenson, A.W., Barnea, Z., 40, 530 (1984)

Fixed Slit Intensity %

89.18

0 15 30 45 60 75 2 θ°

2θ	Int-f	h	k	l	2θ	Int-f	h	k	l	2θ	Int-f	h	k	l
23.881	999 *	1	0	0	52.148	4	0	0	4	74.265	2	2	0	4
25.391	589	0	0	2	55.878	63	2	0	2	76.733	65	3	0	0
27.097	752	1	0	1	58.129	4	1	0	4	79.433	145	2	1	3
35.135	329	1	0	2	63.882	176	2	0	3	82.363	52	3	0	2
41.998	691	1	1	0	66.377	59	2	1	0	82.493	16	0	0	6
45.809	647	1	0	3	67.878	58	2	1	1	86.913	52	2	0	5
48.886	101	2	0	0	69.097	8	1	1	4	87.419	11	1	0	6
49.716	394	1	1	2	71.900	110	1	0	5	89.178	1	2	1	4
50.698	95	2	0	1	72.294	47	2	1	2					

Figure.6- XRD pattern CdSe JCPDS CAS No.77-2307

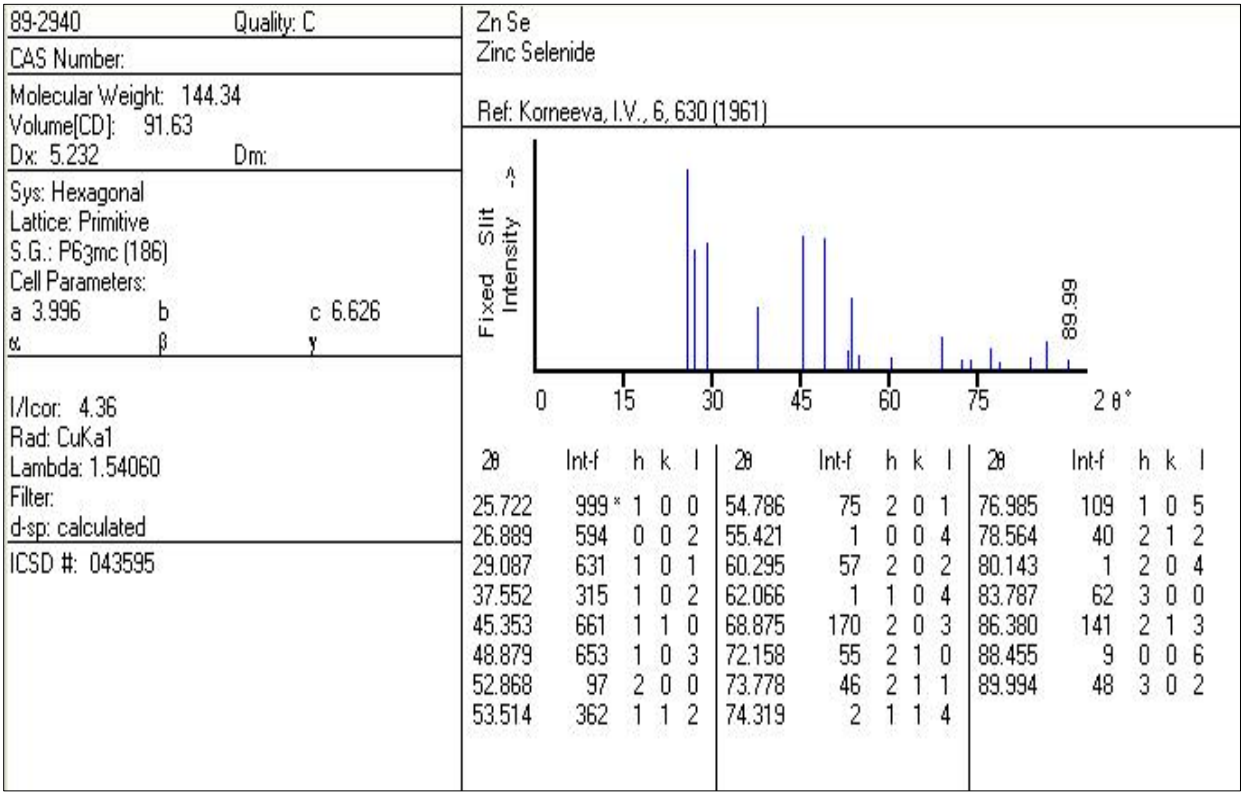

89-2940 Quality: C

CAS Number:

Molecular Weight: 144.34
Volume[CD]: 91.63
Dx: 5.232 Dm:

Sys: Hexagonal
Lattice: Primitive
S.G.: P63mc (186)
Cell Parameters:
a 3.996 b c 6.626
α β γ

I/Icor: 4.36
Rad: CuKa1
Lambda: 1.54060
Filter:
d-sp: calculated

ICSD #: 043595

Zn Se
Zinc Selenide

Ref: Korneeva, I.V., 6, 630 (1961)

Fixed Slit Intensity %

89.99

0 15 30 45 60 75 2 θ°

2θ	Int-f	h	k	l	2θ	Int-f	h	k	l	2θ	Int-f	h	k	l
25.722	999 *	1	0	0	54.786	75	2	0	1	76.985	109	1	0	5
26.889	594	0	0	2	55.421	1	0	0	4	78.564	40	2	1	2
29.087	631	1	0	1	60.295	57	2	0	2	80.143	1	2	0	4
37.552	315	1	0	2	62.066	1	1	0	4	83.787	62	3	0	0
45.353	661	1	1	0	68.875	170	2	0	3	86.380	141	2	1	3
48.879	653	1	0	3	72.158	55	2	1	0	88.455	9	0	0	6
52.868	97	2	0	0	73.778	46	2	1	1	89.994	48	3	0	2
53.514	362	1	1	2	74.319	2	1	1	4					

Figure.7- XRD pattern ZnSe JCPDS CAS No.89-2940

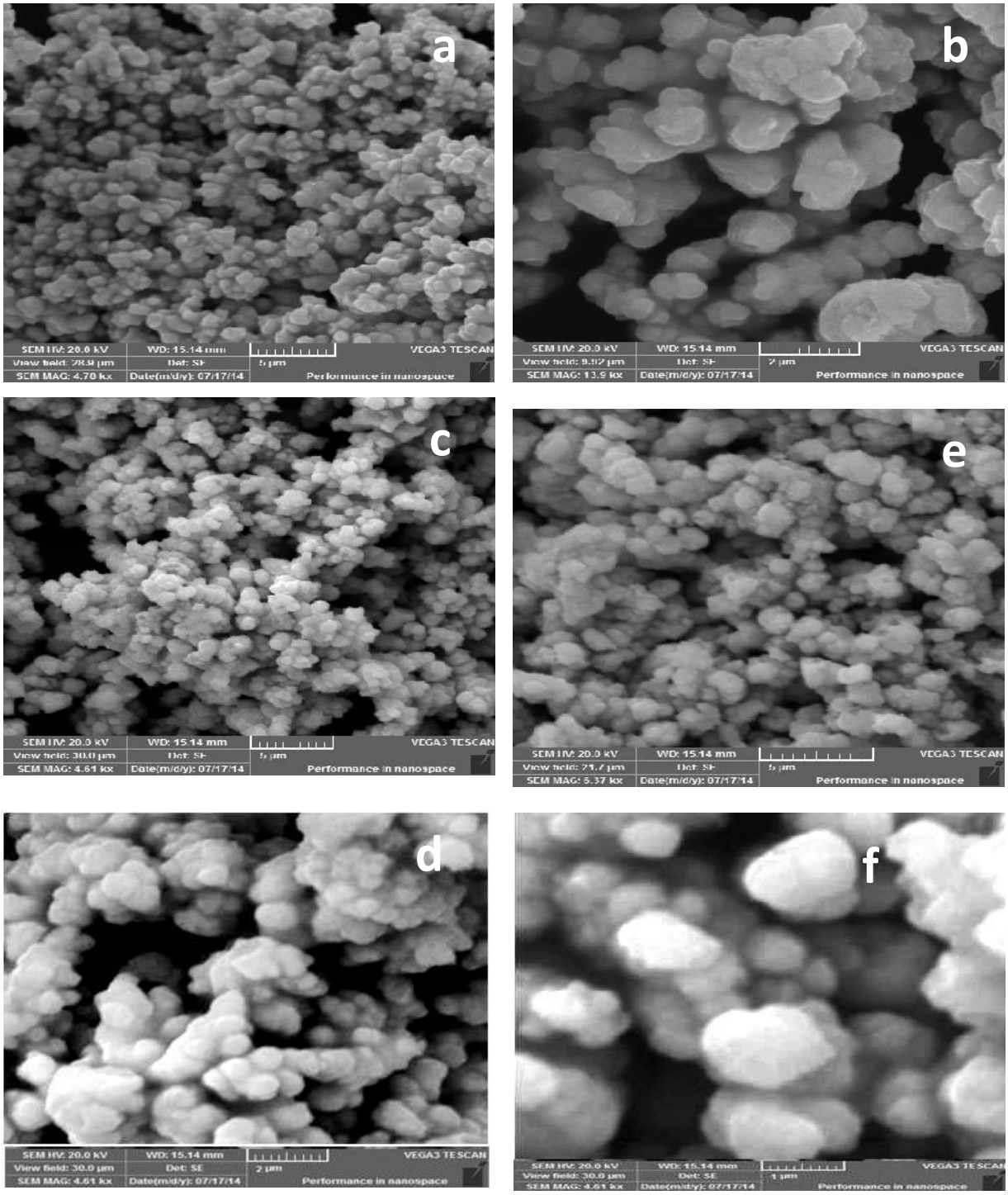

Figure 8- SEM images of SeNPs, Where a,b,c,d,e,f are the SeNPs synthesized from $[Hmim]CH_3CH(OH)COO^-$, $[Heim]CH_3CH(OH)COO^-$, $[Hbim]CH_3CH(OH)COO^-$, $[Hmim]CH_2(OH)COO^-$, $[Heim]\ CH_2(OH)COO^-$, $[Hbim]\ CH_2(OH)COO^-$) respectively.

3.5.Scanning electron microscope(SEM) analysis

The SEM analysis of SeNPs revealed that all the synthesized SeNPs possess spherical shapes.(Figure 8) .It was evident from the SEM images of CdSe and ZnSe (figure- 9 and figure- 10 respectively)that CdSe and ZnSe had pebbleand cluster like structure respectively.

The EDAX analysis confirmed that the SeNPs contained pure selenium without elemental impurities (figure-11).In addition the chemical composition of CdSe and ZnSe was also confirmed by EDAX analysis as shown in figure-12and 13 respectively.

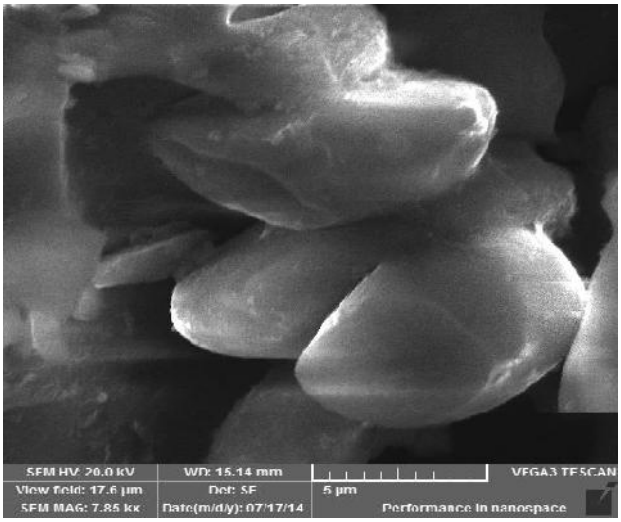

Figure.9-SEM image of CdSe nanoparticle

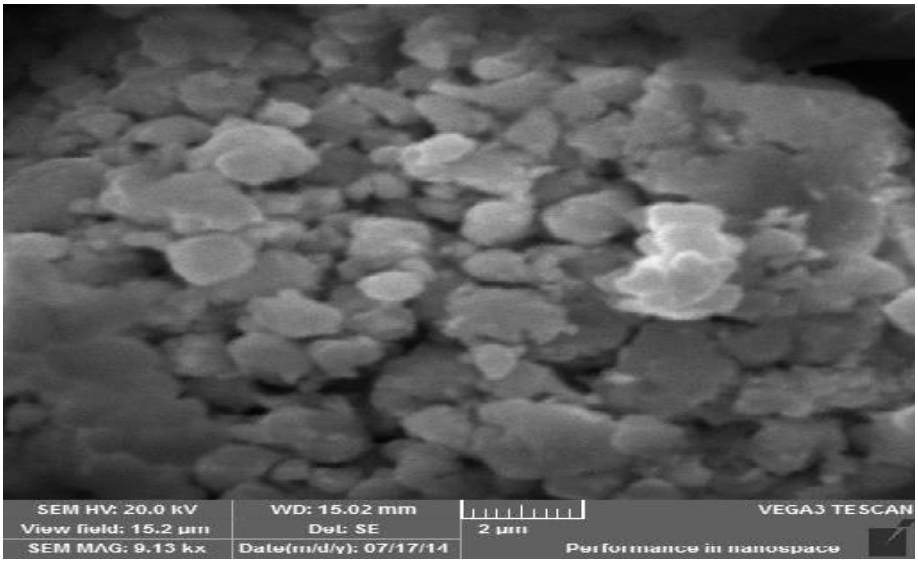

Figure.10-SEM image of ZnSe nanoparticle

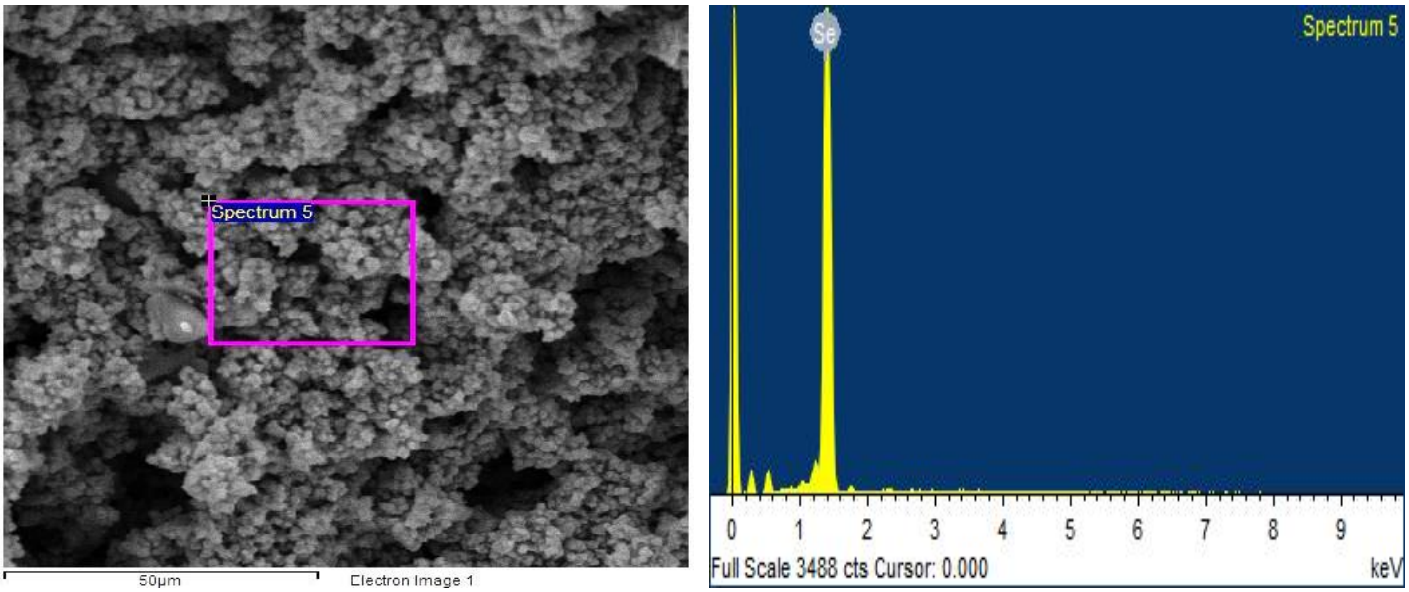

Figure 11- EDAX analysis of SeNPs

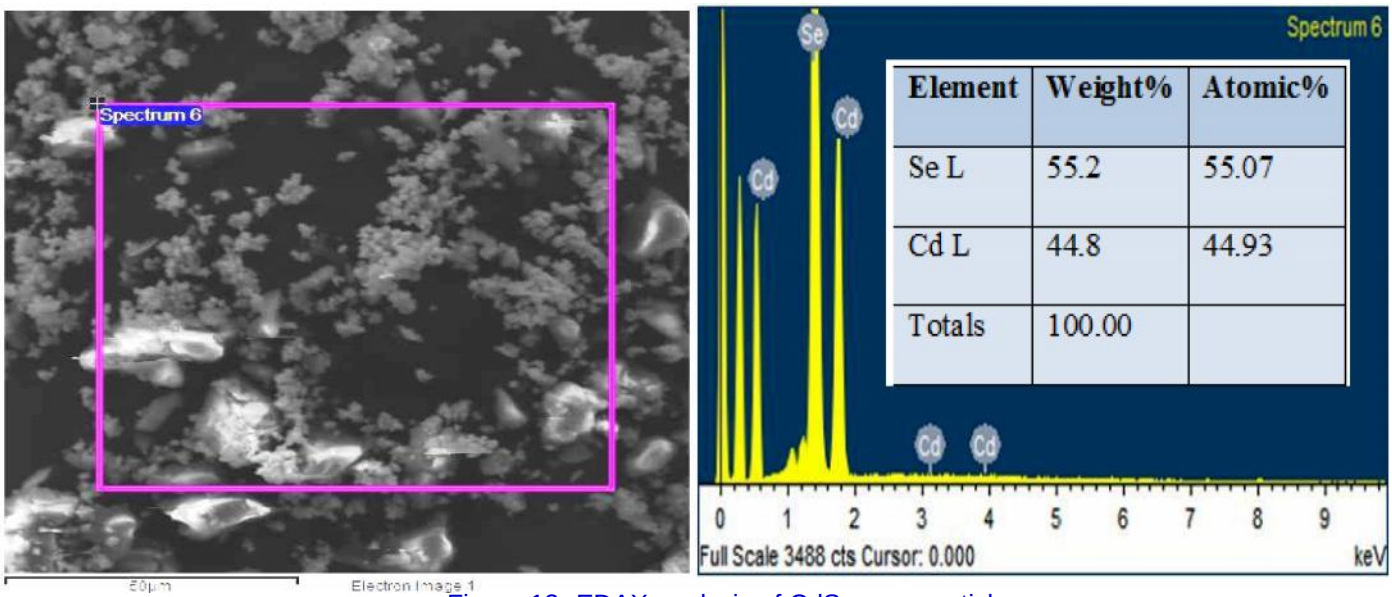

Figure.12- EDAX analysis of CdSe nanoparticle

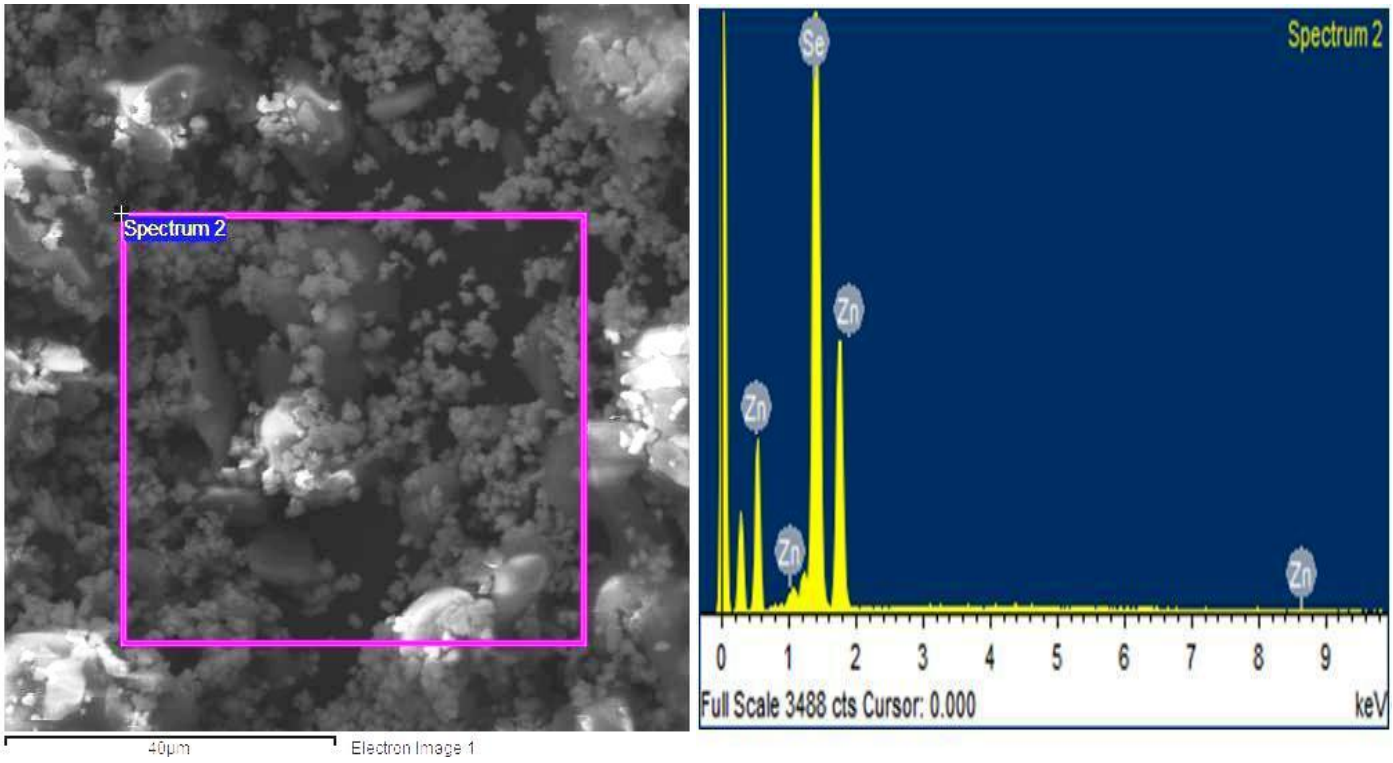

Figure.13- EDAX analysis of ZnSe nanoparticle

3.6. Transmission Electron Microscope (TEM) Analysis

TEM analysis provides actual size, shape and surface topography of the nanopartices. A typical TEM image of SeNPs shown in figure-14 a&b. The spherical shape of the particles visible in the TEM image shows a size distribution around 20nm.In addition, the TEM images of CdSe (figure -15a& b), ZnSe (figure -16 a& b) confirm their pebbleand cluster morphology respectively. Figure 14c,15c and16c shows the selected area electron diffraction (SAED) patterns of SeNPs, CdSe and ZnSe respectively. The SAED patterns confirm the single crystal nature of the nanoparticle.

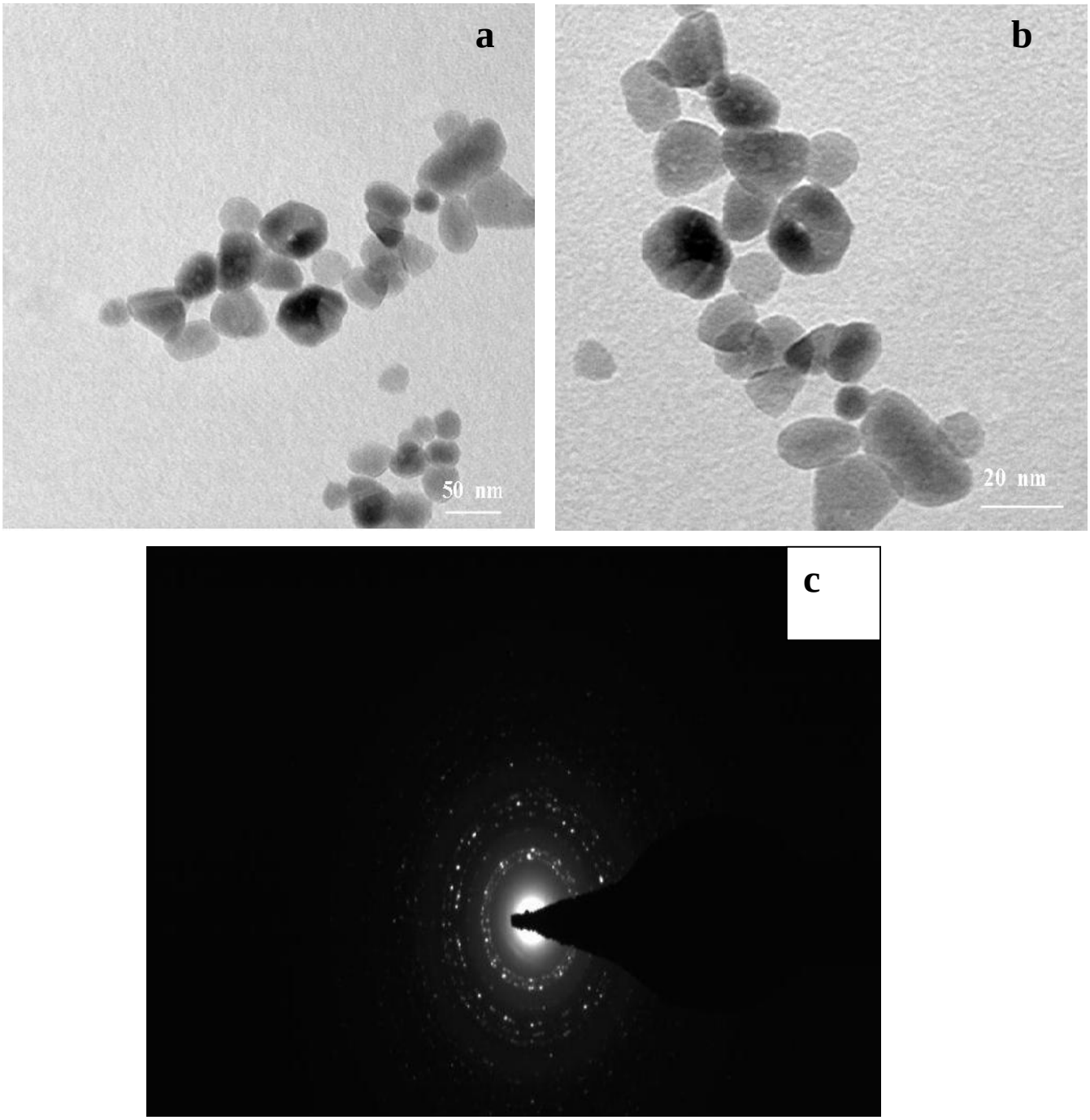

Figure. 14- TEM images of SeNPs

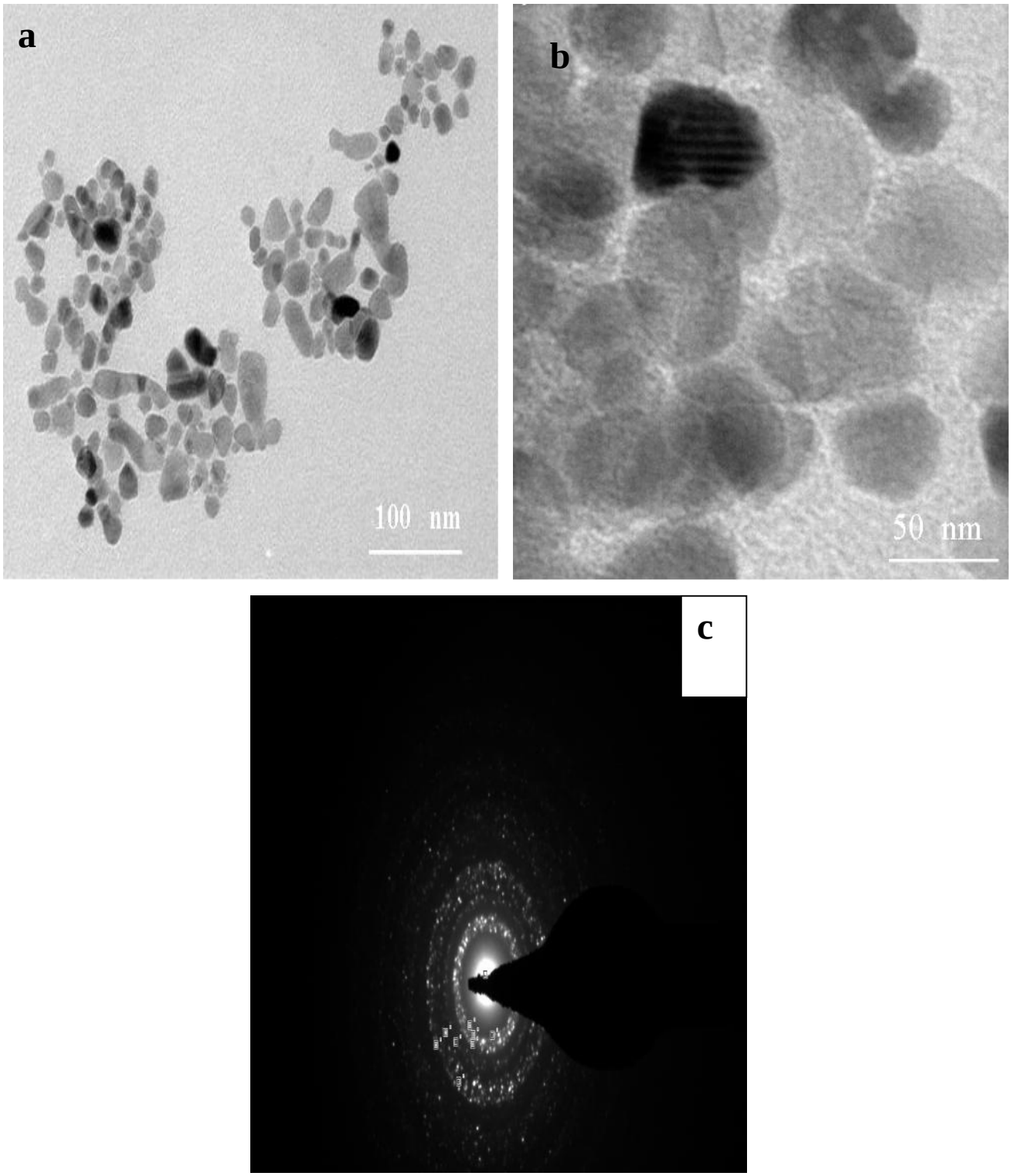

Figure 15- TEM images of CdSe

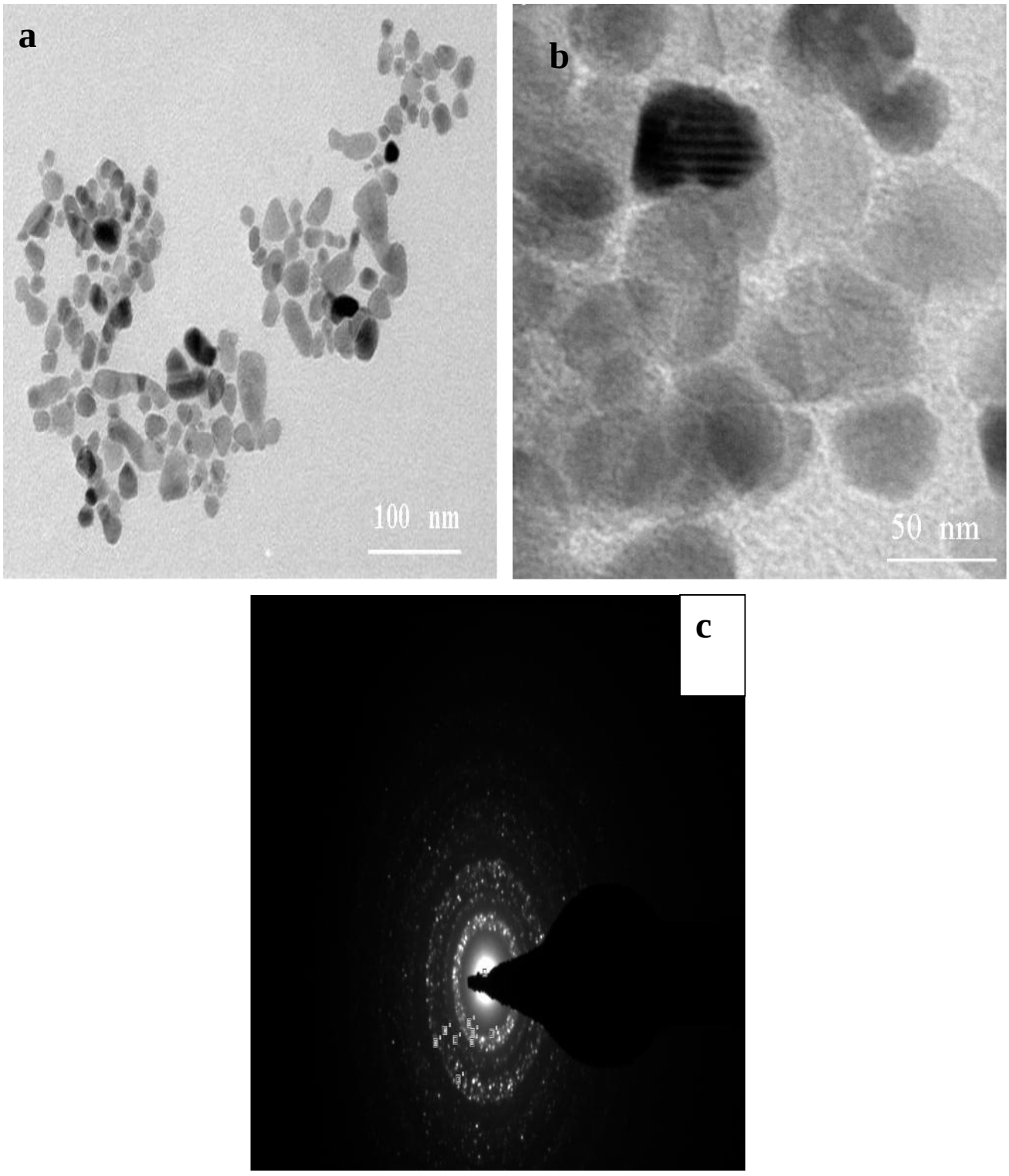

Figure.16-TEM images of ZnSe

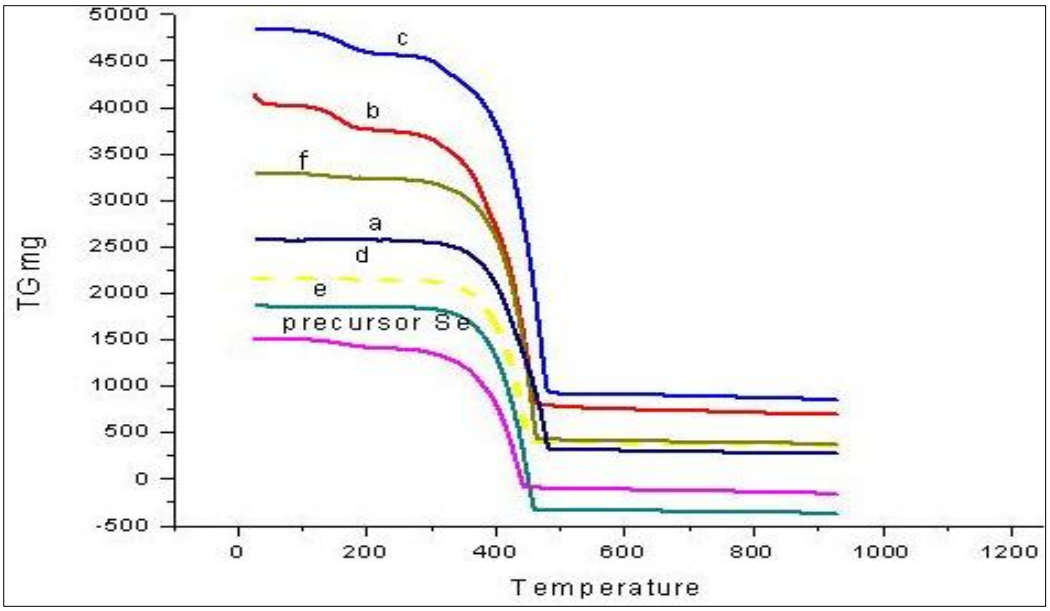

Figure.17- TGA analysis of SeNPs, Where a,b,c,d,e,f are the SeNPs synthesized from [Hmim]$CH_3CH(OH)COO^-$, [Heim]$CH_3CH(OH)COO^-$, [Hbim]$CH_3CH(OH)COO^-$, [Hmim]$CH_2(OH)COO^-$,[Heim] $CH_2(OH)COO^-$, [Hbim] $CH_2(OH)COO^-$ respectively

3.7.Thermogravimetric analysis(TGA) and Differential thermal analysis(DTA)

The thermal analysis(TGA) of SeNPs proved stableness and it started to decompose between 260-330^oC where as the initial selenium precursor at 240^oC(figure-17).Thus the SeNPS possess higher thermal stability. Since the SeNPs synthesized using [Hbim] $CH_2(OH)COO^-$were strongly stabilized possessing very high thermal decomposition temperature of 330^oCthereby attaining higher thermal stability. (Figure- 18).

From the DTA measurement itis obvious that the melting point of SeNPs lie between218-220^oC (figure-18)while precursor selenium had 222.2^oC.Themelting point of solid materials can be reduced to a higher extend when processed as nanostructures [30]. As a result of lower particle size the SeNPs synthesized by [Hbim] $CH_2(OH)COO^-$) acquires low melting point at about 218^oC.

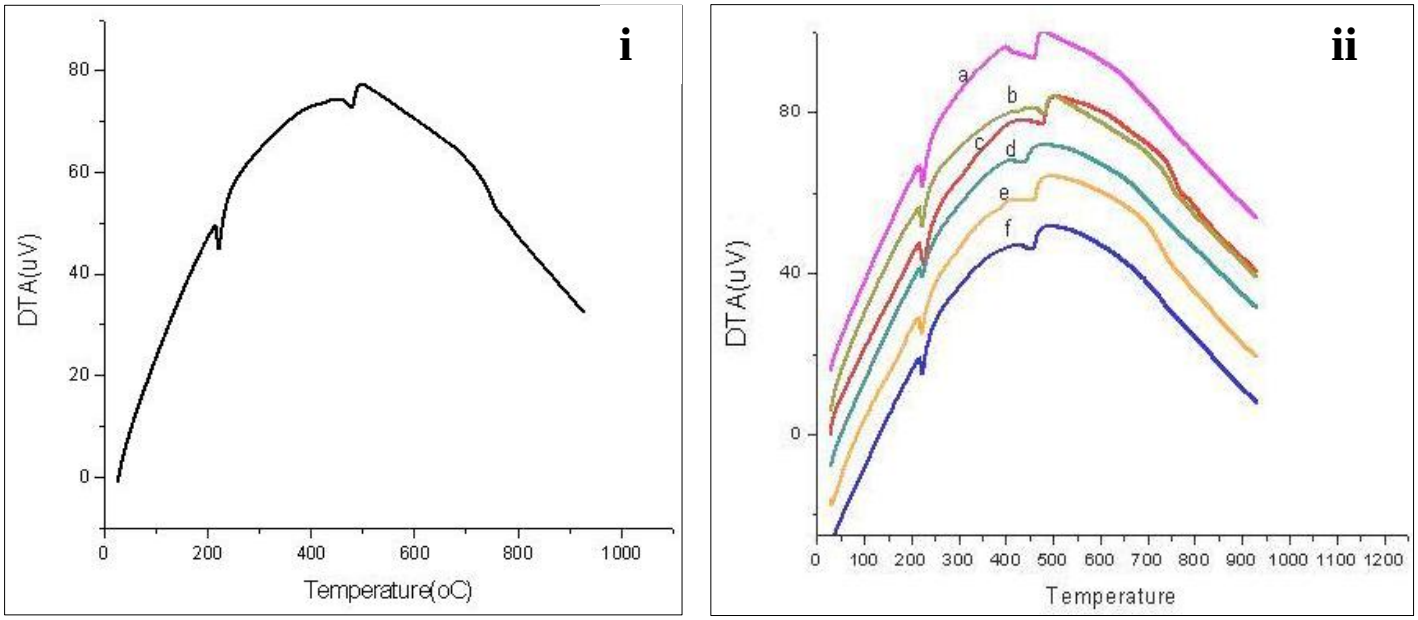

Figure- 18..DTA analysis of precursor selenium(i) and SeNPs(ii)
Where a,b,c,d,e,f are the SeNPs synthesized from [Hmim]$CH_3CH(OH)COO^-$, [Heim]$CH_3CH(OH)COO^-$, [Hbim]$CH_3CH(OH)COO^-$,[Hmim]$CH_2(OH)COO^-$,[Heim] $CH_2(OH)COO^-$, [Hbim] $CH_2(OH)COO^-$ respectively.

4. CONCLUSION

The SeNPs were synthesized successfully using six different imidazolium protic ionic liquids. The XRD measurements and TEM analysis confirm that the sizes of synthesized SeNPs were found to be in a range of 19-24 nm. The morphology of the SeNPs was identified by means of SEM and TEM analysis and revealed that the SeNPs were spherical in shape. The EDAX analysis of SeNPs confirmed that the presence of elemental selenium without any impurities. Furthermore the synthesized SeNPs hadan increased optical energy band gap and were blue shifted from the initial selenium precursor. Thus SeNPs provided a scope of optical applications. The thermal stability of the SeNPs could be confirmed by TGA measurements and the synthesized SeNPs possess low melting point around 218^{o}C

The chalcogenide nanomaterials like CdSe and ZnSe were synthesized by SeNP obtained from [Hbim] $CH_2(OH)COO^-$) as a precursor. The synthesized CdSe and ZnSe had a particle size of 29.9678 nm and 22.7283 nm respectively. The morphology of CdSe and ZnSe were confirmed by SEM,TEM analysis and the elemental composition was proven by their EDAX analysis. Hence the synthesized SeNPs may serve as a template to generate important nanomaterials.

5. REFERENCES

[1] S. Gabriel and J. Weiner, 2669-2679 (1888).
[2] N. V. Plechkova, R. D. Rogers and K. R. Seddon, Eds., 472(2009).
[3] J. S. Wilkes, P. Wasserscheid and T. Welton, 1-6(2007).
[4] J. D. Holbrey, R. D. Rogers, R. A. Mantz, P. C. Trulove, V. A. Cocalia, A. E. Visser, J. L. Anderson, J. L. Anthony, J. F. Brennecke, E. J. Maginn, T. Welton and R. A. Mantz, 57-174 (2007).
[5] S. Sowmiah, C. I. Cheng and Y.-H. Chu, 74-95 (2012).
[6] M. J. A. Shiddiky and A. A. J. Torriero, 1775-1787 (2011).
[7] C. M. Gordon, 101-117(2001).
[8] F. Karadas, M. Atilhan and S. Aparicio, “5817-5828(2010).
[9] T. L. Greaves and C. J. Drummond, 206-237(2007).
[10] H. Markusson, J.-P.Belières, P. Johansson, C. A. Angell and P. Jacobsson, 8717-8723(2007).
[11] L. Timperman, P. Skowron, A. Boisset, H. Galiano, D. Lemordant, E. Frackowiak, F. Beguin and M. Anouti, 8199-8207 (2012).
[12] Z. Du, Z. Li, S. Guo, J. Zhang, L. Zhu and Y. Deng, 19542- 19546 (2005).
[13] M. S. Miran, H. Kinoshita, T. Yasuda, M. A. B. H. Susan and M. Watanabe, 12676-12678 (2011).
[14] M. Yoshizawa, W. Xu and C. A. Angell, 15411-15419 (2003).
[15] C. F. Poole, 49-82 (2004). .
[16] W. Wang, L. Shao, W. Cheng, J. Yang and M. He, 337-341(2008).
[17] S.-Y. Lee, A. Ogawa, M. Kanno, H. Nakamoto, T. Yasuda and M. Watanabe, 9764-9773(2010).
[18] A. Fernicola, S. Panero and B. Scrosati, 591-595(2008).
[19] H. Ye, J. Huang, J. J. Xu, N. K. A. C. Kodiweera, J. R. P. Jayakody and S. G. Greenbaum, 651-660,(2008)..
[20] Jagminas, I. Gailiute, G. Niaura, R. Giraitis, Chemija., 16 ,15(2005).
[21] X. Cao, Y. Xie, S. Zhang, F. Li, Adv. Mater., 16,649(2004).
[22] T. W. Smith, R. A. Cheatham, Macromolecules, 13,1203(1980).
[23] D.H. Son, S.M. Hughes, Y. Yin, A. P. Alivisatos, Science, 306(2004), 1009.
[24] P. H. C. Camargo, Y. H. Lee, U. Jeong, Z. Zhou, Y. Xia, Langmuir,23, 2985(2007).
[25] B.Meenatchi , V.Renuga,International Journal of Advanced Research,2,1107(2014).
[26] M. Antonietti, D. Kuang, B. Smarsly, Y. Zhou, Angew.Chem. Int. Ed., 43 ,4988(2004).
[27] S.M .Sze “ Physics of semiconductor devices (2nd edition)”,Wiley,Delhi(1981).
[28] Ludolph , M. A. Malik ,Chem.Commun.,1849-1850(1998).
[29] J.A. Eastman, L.J. Thompson, B.J. Kestel, Phys. Rev. B,48 ,84(1993).
[30] R. Ingole, S. R. Thakare, N.T. Khati, A. V. Wankhade, D. K. Burghate , Chalcogenide Letters ,7, 485(2010).